Presented at GNSS 2004
The 2004 International Symposium on GNSS/GPS

Sydney, Australia
6–8 December 2004

Overbounding SBAS and GBAS Error Distributions with Excess-Mass Functions

J. Rife
Stanford University; Palo Alto, CA 94305
jrife@stanford.edu

T. Walter
Stanford University; Palo Alto, CA 94305
twalter@stanford.edu

J. Blanch
Stanford University; Palo Alto, CA 94305
blanch@stanford.edu

ABSTRACT

Safety-of-life GNSS augmentation systems must provide bounds on the probability with which hazardous navigation errors occur. This paper develops conservative bounding methods both for space-based augmentation systems (SBAS) and for ground-based augmentation systems (GBAS) by using excess-mass functions. The excess-mass concept, which employs conservative bounding functions with integrated density greater than unity, is applied to develop two new bounding strategies, of which the first focuses on probability density functions (EMP overbounding) and the second on cumulative distribution functions (EMC overbounding). These strategies can bound arbitrary error distributions, even those that are asymmetric, multimodal, or non-zero mean.

To compare the two strategies to each other, and to existing methods such as paired-CDF overbounding and moment overbounding, a set of metrics are introduced to evaluate overbound performance given anomalies in the actual error distribution. These performance metrics provide a basis for application-specific trade studies that would balance the availability benefits of various overbounding methods against required modifications to the broadcast signal and protection limits. In the generic case, assuming identical error sources for all satellites and neglecting broadcast-message bandwidth constraints, the performance metrics favour the EMC approach, which tightly bounds unknown biases and heavy-tailed errors. The major drawback of the EMC approach is its sensitivity to outliers in sampled error distributions.

KEYWORDS: Overbounding, CDF, PDF, Differential GPS, Augmentation System.

1. INTRODUCTION

In a differential GNSS augmentation system, fixed-base ground stations make estimates of satellite ranging errors and broadcast these corrections to mobile users. This strategy improves accuracy because the dominant sources of measurement error correlate strongly between ground stations and proximate mobile users. Secondary error sources, however, including ground or airborne multipath, ionospheric gradients, tropospheric gradients, radio frequency interference, and thermal noise, introduce errors that are uncorrelated between the ground station and the mobile user. To establish system integrity, the augmentation system broadcasts a bound on these secondary errors. The mobile user can thereby generate confidence limits for navigation accuracy to assess the threat of hazardously large errors.

The broadcast error bound must conservatively represent the actual error distribution in order to guarantee integrity. For augmentation systems that transmit pseudorange corrections, this conservatism must apply both in the range domain and in the position domain. The position-domain requirement stems from the need to form an error envelope, called a protection limit (PL), around the mobile user's location. For safe operations, the PL must remain smaller than a specified alert limit (AL). A conservative PL can only be established for a pseudorange-correction system if each broadcast ranging error is individually bounded. A bound that provides conservatism in both the range and position domains is referred to as an overbound.

Many proposed bounding strategies fail to provide conservatism across both the range and position domains (Ober *et al.*, 2001). An example of such a deficient strategy is called the tail bounding method. The tail bounding strategy, derived from the PL requirement, defines a conservative distribution as one with greater probability mass in its tail than the actual error distribution. Mathematically, a tail bound is defined to have a cumulative distribution function (CDF), G_b, greater than the actual error distribution, G_a, when evaluated at the protection limit, PL.

$$G_b\left(x=-PL\right)\geq G_a\left(x=-PL\right)\ \ \&\ \ \left(1-G_b\left(x=PL\right)\right)\geq\left(1-G_a\left(x=PL\right)\right) \tag{1}$$

These inequalities define a conservative position-domain bound in accordance with the PL concept. Unfortunately, tail bounding of individual range-domain error distributions does not guarantee tail bounding in the position domain. Even if the tail-bounding relationship is formulated using a probability density function (PDF) rather than a CDF, as described by the following equation, tail bounding still fails to guarantee a position-domain overbound even when all range-domain error distributions are similarly tail-bounded.

$$g_b\left(x\right)\geq g_a\left(x\right),\ \ \forall\left|x\right|>PL \tag{2}$$

In this PDF-based tail bounding equation, and throughout this paper, lower-case variable names indicate PDFs, in contrast with upper-case variable names, which indicate CDFs.

DeCleene (2000) introduced the first true overbound. DeCleene's strategy, called CDF overbounding, defined the overbounding distribution, G_o, as one with more tail mass than the actual distribution, G_a, for all values along the real axis.

$$\begin{aligned} &G_o\left(x\right)\geq G_a\left(x\right),\ \ \forall G_a<\tfrac{1}{2}\\ &G_o\left(x\right)\leq G_a\left(x\right),\ \ \forall G_a\geq\tfrac{1}{2}\end{aligned} \tag{3}$$

In contrast with (1) and (2), the CDF overbound definition does not explicitly reference the PL. CDF bounding thereby avoids a pitfall of tail bounding, since the tails of the position-

domain error are, in fact, formed from the spans of the range-domain error distributions, and not merely from their tails. To validate range-to-position conversion, the CDF overbound and the actual error distribution must obey certain shape restrictions. Specifically, G_o and G_a must be symmetric, unimodal and zero-mean.

More recent overbounding efforts have focused on relaxing these shape constraints. This paper introduces two new overbounding strategies, with no restrictions on symmetry, local modes or nonzero means. The new strategies both rely on the notion that the overbound, unlike the actual error distribution, need not integrate to a total probability mass of one. Thus, an excess-mass PDF (EMP) bound can be defined with a cumulative density of

$$K = \int_{-\infty}^{\infty} g_o(x)dx \geq 1 \ . \tag{4}$$

Likewise, an excess-mass CDF (EMC) bound can be defined with a limiting value above one:

$$K = \lim_{x \to \infty} G_o(x) \geq 1 \ . \tag{5}$$

For inspiration, both concepts draw on the observation by DeCleene (2004) that the CDF bounding method does not restrict the total mass of the overbounding function.

Section 2 introduces the EMP and EMC bounding strategies in more detail. For context, the section also surveys other research into overbounds free of distribution-shape constraints. These existing strategies comprise moment bounding, a strategy developed and patented by Raytheon (2002) for use with WAAS, and paired-CDF bounding, a strategy proposed by Rife *et al.* (2004a) for use with LAAS.

Choice among these various overbounding strategies provides flexibility in integrity design for a GPS augmentation system. To enable quantitative comparison, Section 3 develops a total inflation metric to distinguish the various options. Section 4 applies the total inflation metric to assess performance in bounding nonideal error distributions. The performance analysis characterizes the inflation requirements imposed by unknown biases, heavy-tail error distributions, and outliers in sampled data. These performance comparisons provide a basis for future application-specific trade studies. For the generic case, with unrestricted bandwidth and identical error sources for all satellites, EMC bounding offers the best overall capability for bounding nonideal error distributions.

2. EXCESS-MASS OVERBOUNDING

This section provides a survey of overbounding strategies, and in particular of those strategies not constrained by implicit restrictions on asymmetry, multiple modes, or nonzero means. Previous researchers have described two methods in this class: moment bounding and paired-CDF bounding. This section adds two new overbounding strategies to the list. These methods, called excess-mass CDF (EMC) and excess-mass PDF (EMP) bounding, both employ overbounding functions with cumulative density greater than one. Figure 1 provides a graphical summary of these methods.

2.1 Paired-CDF Overbounding

Of the two previously existing overbounding strategies with no shape restrictions, the paired-CDF overbound most closely resembles DeCleene's original method. The paired-bound

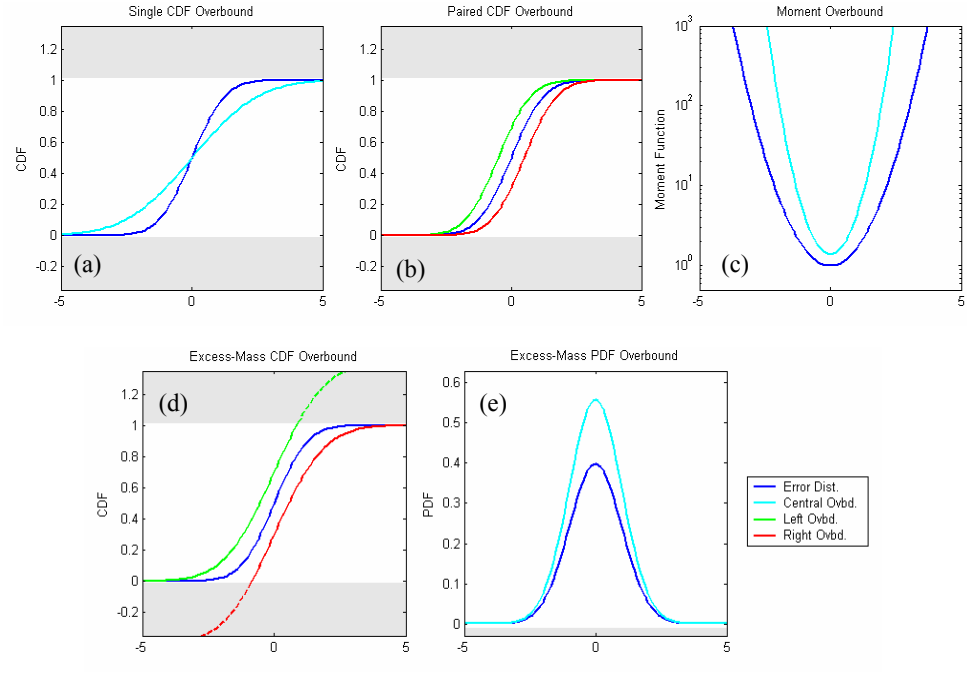

Figure 1. Overbounding Strategies. (a) The first method, single-CDF Bounding, is restricted to symmetric, unimodal, zero-mean distributions. The subsequent four methods, including the excess-mass methods introduced in this paper, do not suffer distribution shape constraints. These methods include (b) paired-CDF, (c) moment, (d) EMC and (e) EMP overbounding.

strategy modifies the single-CDF overbound to avoid the shape restrictions associated with (3). These restrictions arise because the overbound and the actual error distribution must both share a common median. The median constraint vanishes if the bound is broken into two parts, one to the left (G_L) and one to the right (G_R) of the actual distribution.

$$\begin{aligned} G_L(x) &\geq G_a(x), \quad \forall x \\ G_R(x) &\leq G_a(x), \quad \forall x \end{aligned} \quad . \tag{6}$$

A proof of range-to-position domain conservatism for this method is presented in (Rife *et al.*, 2004a). The proof allows for both the overbound and the actual distribution to be asymmetric, multimodal and biased from a zero-mean.

The bounding functions, G_L and G_R, should be selected to provide a tight bound for the actual error distribution. For GNSS augmentation applications, differential correction errors are approximately Gaussian. To take advantage of this near-Gaussian structure, left and right bounds can be defined as shifted normal distributions, $\mathcal{N}$, with identical standard deviation, σ_a, displaced in opposite directions by a bias, b.

$$\begin{aligned} G_L(x) &= \int_{-\infty}^{x} \mathcal{N}(-b, \sigma_a)\, dx \\ G_R(x) &= \int_{-\infty}^{x} \mathcal{N}(b, \sigma_a)\, dx \end{aligned} \tag{7}$$

As illustrated in Figure 1b, this pair of Gaussians encloses an envelope. Any distribution within this envelope is overbounded according to (6).

2.2 Moment Overbounding

Instead of working directly with a PDF or a CDF, moment overbounding operates in the moment domain. The moment-generating operation is an integral transform similar to the Laplace transform.

$$m(t) = \int_{-\infty}^{\infty} e^{tx} g(x) dx \tag{8}$$

Everywhere along the real axis, a moment overbound, $m_o(t)$, must have a greater value than the transform for the actual error distribution, $m_a(t)$.

$$m_o(t) \geq m_a(t), \ \forall t \tag{9}$$

It is straightforward to prove that the position-domain error is moment-overbounded by the product of range-domain moment overbounds, so long as all moment transforms converge. The probability distribution recovered by applying an inverse transform to the moment bound, however, is not guaranteed to be a position-domain bound. Consequently, Raytheon (2002) derived an upper bound for tail probability for any given moment bound, $m_o(t)$.

$$G_a(x = PL) \leq m_o(t) \exp(-PL \cdot t) \ . \tag{10}$$

This final conversion step makes moment bounding slightly inefficient in comparison with other methods, which bound directly in the probability domain.

For a Gaussian distribution, the moment bound takes the following form:

$$m(t) = \int_{-\infty}^{\infty} e^{tx} K \cdot \mathcal{N}(0, \xi\sigma_a) dx = K e^{\frac{1}{2}(\xi\sigma_a t)^2} \ . \tag{11}$$

The factor K is a total-mass parameter that allows the overbounding function to have an integral greater than one. The parameter ξ is a sigma-inflation, which permits the overbound standard deviation to be greater than that for the actual distribution. For a valid overbound, both the K and ξ parameters must be greater than one.

2.3 Excess-Mass CDF Overbounding

This section introduces the excess-mass CDF (or EMC) overbound, the first of two new overbounding techniques based on excess-mass functions. Allowing the overbounding distribution to have a total mass, K, greater than one provides an extra degree of freedom to enable sharp bounding of actual error distributions, particularly under nonideal circumstances. The excess-mass parameter also helps relate CDF bounds to moment bounds, which already incorporate a K-parameter, as described by (11).

The EMC bound is a generalization of the paired bound defined by (6). Specifically, the right bound is redefined to permit negative values and to guarantee a maximum value of one.

$$G_R^*(x) = \int_{-\infty}^{x} g_R(x) dx + (1 - K) = 1 - \int_{x}^{\infty} g_R(x) dx \tag{12}$$

With this reformulation of the right bound, a paired EMC bound can be defined as:

$$G_L(x) \geq G_a(x), \ \forall x$$
$$G_R^*(x) \leq G_a(x), \ \forall x \quad . \tag{13}$$

The proof of conservatism through the range-to-position transformation is otherwise identical to that for paired CDF bounding (Rife *et al.*, 2004a). By incorporating excess mass, the EMC approach gains a degree of freedom, as evidenced by the 3 parameters of the Gaussian EMC: K, the total mass parameter, ξ, the sigma-inflation parameter, and b, the unknown bias shift.

$$G_L(x) = \int_{-\infty}^{x} K \cdot \mathcal{N}(-b, \xi\sigma_a)\, dx$$
$$G_R^*(x) = \int_{-\infty}^{x} K \cdot \mathcal{N}(b, \xi\sigma_a)\, dx + (1-K) \tag{14}$$

As a special case, the EMC technique permits robust overbounding using a single CDF. In contrast with the CDF bound defined by (3), the single-EMC bound handles asymmetry, multiple modes and nonzero mean. This shape robustness results because left and right bounds differ for an excess-mass function when integrated according to (14). Figure 1d illustrates the left and right integrals for a Gaussian single-EMC bound ($b = 0$, $K > 1$). The envelope defined by the left and right integrals of the excess-mass function resembles the envelope defined by the Gaussian paired CDFs shown in Figure 1b.

2.4 Excess-Mass PDF Overbounding

Excess-mass functions also enable a second new overbounding strategy, called excess-mass PDF (EMP) overbounding. This new strategy revives the concept of PDF bounding. The pursuit of overbounding strategies based on probability density functions was largely abandoned after early successes in CDF bounding displaced the PDF tail-bounding approach described by (2). PDF overbounding remains an attractive approach, however, because of its intuitive nature.

Using the excess-mass approach, a PDF bound, g_o, can be defined as a function everywhere greater than the actual error PDF, g_a.

$$g_o(x) \geq g_a(x), \ \forall |x| \ . \tag{15}$$

This definition guarantees position-domain bounding of independent error sources that are EMP bounded in the range-domain. The appendix offers a proof of this range-to-position domain conservatism. For practical applications, for which the actual distribution is nearly Gaussian, a Gaussian form of the EMP bound is defined as

$$g_o(x) = K \cdot \mathcal{N}(0, \xi\sigma_a) \ . \tag{16}$$

The excess-mass parameter is critical here in establishing robustness. If the sigma-inflation parameter, ξ, were increased without also increasing the mass parameter, K, the resulting EMP function would not bound a unity-sigma, unity-mass Normal distribution. Section 3.2 explores the constraint relationship between the K and ξ parameters in more detail.

The EMP bound is the most restrictive of the bounds in this section. If (15) holds, then it follows that (9) and (13) also hold. Thus the existence of a Gaussian EMP bound also guarantees the existence of a Gaussian moment bound and of a Gaussian EMC bound.

3. OVERBOUND-BASED PROTECTION LEVEL DEFINITION

The protection level (PL) represents a confidence limit on the position solution used for navigation. If the PL grows wider than the alert limit (AL), which defines the boundaries for safe navigation, an alarm triggers to warn the pilot of a possible hazard. In this sense, the PL equation provides an instantaneous test for quality of the satellite geometry observed by a mobile user. For this reason, unnecessary conservativism in the definition of the PL results in a reduction of system availability due to the exclusion of marginal satellite geometries.

This section derives PL expressions for each of the overbounding methods previously described. A total inflation factor metric, based on these PL expressions, is also developed. This metric will be employed subsequently to assess excess PL margin and, thereby, to provide an indication of the availability penalty associated with each overbounding method.

3.1 PL Equations for Paired CDF, Moment, EMC and EMP Overbounding

In the general case, the protection level is defined by inverting an overbound and evaluating the inverted function at an allowed double-tail fault probability. This probability of hazardously misleading information, P_{HMI}, is a specification that differs among augmentation applications (but is commonly in the range of 10^{-7} to 10^{-9}).

$$PL = G_o^{-1}(\tfrac{1}{2} P_{HMI}) \tag{17}$$

The magnitude of the PL depends on the form of the overbounding CDF, G_o. This section defines a PL expression for each of the Gaussian overbounds described in the previous section, including paired-CDF, moment, EMC and EMP overbounding. These PL expressions are derived assuming homogeneous error sources. For the purposes of comparison, all PL expressions are referenced to a baseline, PL_0, which describes an unbiased, uninflated Gaussian distribution:

$$PL_0 = A_0 \sigma_p \quad \text{with} \quad \sigma_p = \sqrt{\sum_N S_i \sigma_{o,i}} \quad \text{and} \quad A_0 = \sqrt{2} erfc^{-1}(P_{HMI}) . \tag{18}$$

Here the position-domain sigma, σ_p, is the root of the sum of the squares of the weighted range-domain sigmas for each of the N observed satellites. The scaling parameter A_0 describes the sigma multiple associated with the integrity probability, P_{HMI}. In WAAS and LAAS implementations, the A_0 parameter is also known as the scaling parameter for fault-free missed detection, K_{ffmd}.

The protection level expressions for Gaussian overbounds established using paired CDF, EMC, and EMP bounding are all closely related. In each case, the position-domain error bound is a modified Gaussian described by a subset of three parameters: sigma inflation factor, ξ, total mass, K, and unknown bias, b. For the case in which all error sources are described by identical values of ξ, K, and b, the modified PL expression is:

$$PL = A\xi\sigma_p + b_p \quad \text{with} \quad b_p = \sum_N |S_i| b_i \tag{19}$$

In this equation, the position-domain bias, b_p, is a sum of weighted range-domain biases. The bias term is zero by default, for EMP bounding, but may be nonzero for EMC and paired-CDF bounding. The scaling parameter, A, is a function of the mass parameter, K, and the

number of satellites, N. When K equals one, as is the case for paired-CDF bounding, A equals A_0.

$$A = \sqrt{2}erfc^{-1}(P_{HMI} / K^N) \tag{20}$$

Equation (19) depends on satellite geometry and the derived sensitivity coefficients, S_i, for each satellite. To remove this dependence, the expression can be simplified using an upper-bound relationship for the vector one-norm (Golub, 1996).

$$b_p \le \sqrt{N}\ \tilde{b}\sqrt{\sum_N S_i^2\sigma_{o,i}^2} \quad \text{where} \quad \tilde{b} = \left|\frac{b_i}{\sigma_{o,i}}\right|_{\max_i} \tag{21}$$

The parameter $\tilde{b}$, which represents the greatest bias-to-sigma ratio over all satellites, replaces the absolute bias, b, as the common parameter that describes all error sources. Invoking (21), the PL expression (19) can be rewritten without an explicit reference to satellite geometry, other than σ_p. The simplified PL expression for paired CDF, EMC and EMP overbounding is

$$PL = \left(A\xi + \sqrt{N}\cdot\tilde{b}\right)\sigma_p \ . \tag{22}$$

For moment bounding, the PL expression resembles (22) with one exception, which involves the conversion of the moment bound into a probability bound according to (10). This conversion results in a scaling factor that is less favourable than (20):

$$A_{moment} = \sqrt{2\ln(2K^N/P_{HMI})}\ . \tag{23}$$

Other than this difference in scaling factor, the moment-bound PL equation is identical to (22), with the bias parameter $\tilde{b}$ set equal to zero.

3.2 Total Inflation Factor

Defining a total inflation factor, Θ, provides a convenient metric to enable overbound comparison. The total inflation factor is the ratio of the overbound-specific PL and the reference PL_0, given by (18). For paired CDF, EMC and EMP overbounding, the total inflation factor is

$$\Theta = PL/PL_0 = \left(A\xi + \sqrt{N}\cdot\tilde{b}\right)\Big/A_0\ . \tag{24}$$

For moment bounding, the total inflation factor is

$$\Theta_{moment} = A_{moment}\xi/A_0 \quad . \tag{25}$$

3.2 Sigma-Relative Bounding

Despite its limitations in bounding asymmetric, multimodal and nonzero mean distributions, the original CDF bounding method, described by (3), possessed a useful property. Namely, a Gaussian CDF automatically bounds all other Gaussian CDFs with smaller standard deviation, σ. This property expresses an intuitive concept, that a wider Gaussian distribution should be more conservative than a narrower one. This intuitive property also holds for moment bounding. Unfortunately, the property does not hold universally for paired CDF, EMC or EMP bounding.

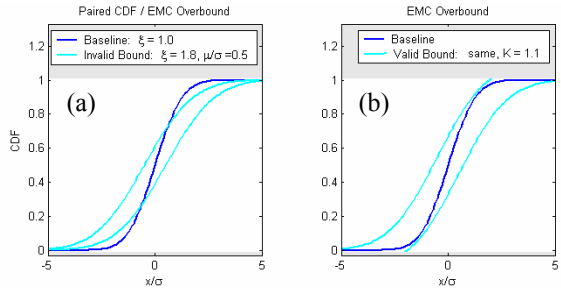

Figure 2. Sigma inflation does not guarantee EMC overbounding

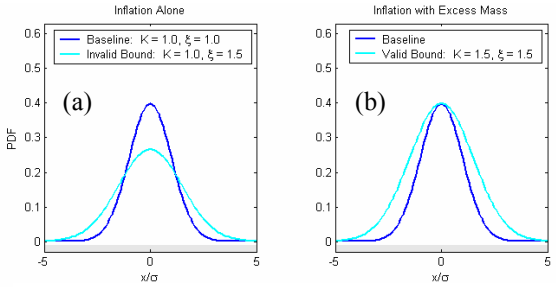

Figure 3. Sigma inflation does not guarantee EMP overbounding

For paired CDF and EMC bounding, the range of valid sigma inflation values, ξ, is limited by the shift parameter, b, and (for EMC bounding) by the total mass, K. Figure 2 illustrates this issue. In the figure, the wide-sigma paired bounds ($\xi = 1.8$) do not overbound a narrow-sigma error distribution ($\xi = 1.0$). The problem is solved in Figure 2b by a slight increase of the excess mass coefficient, K, from 1.0 to 1.1.

For EMP bounding, likewise, sigma inflation does not guarantee conservative overbounding. Figure 3 illustrates a PDF overbound that becomes invalid when the inflation factor increases above unity. Figure 3a shows that a Gaussian with $\xi = 1.5$ does not EMP bound a Gaussian with $\xi = 1.0$. If the inflation factor and the total mass coefficient increase in unison, however, the overbound remains valid, as illustrated by Figure 3b.

These limitations on maximum inflation factor motivate the definition of sigma-relative bounding, a technique that broadens applicability for paired CDF, EMC and EMP overbounding. The sigma-relative concept emphasizes bounding of shape variations relative to a nominal distribution. As such, the overbound sigma is defined to exactly match the sigma of the actual error distribution. The inflation factor, ξ, remains to provide shape flexibility for bounding off-nominal distributions. Of course the exact sigma of the actual distribution is unknown. As long as it is possible to bound the actual sigma, $\sigma_a \in [\sigma_{\min}, \sigma_{\max}]$, however, then a PL can still be constructed by determining the value of σ_a which results in the largest, most conservative PL. By inspection, PL and σ_p are maximized, according to (18), when $\sigma_{a,i} = \sigma_{\max,i}$. In other words, a conservative PL is achieved by simply assuming the worst case standard deviation for each individual ranging source.

The significance of the sigma-relative methodology is twofold. First, the concept preserves the intuitive notion that a wider distribution automatically overbounds a narrower distribution of the same structural form. Second, the methodology decouples the bounding of the actual distribution sigma from the bounding of its off-nominal shape. For paired CDF, EMC and EMP overbounding, the error bound need not be designed to bound a range of sigma values, but merely variations in shape away from a nominal sigma value. The sigma-relative methodology is implicitly assumed in the discussion of the following section.

4. QUANTIFYING THE COMPARISON OF OVERBOUNDS

Although errors for augmented GNSS ranging are often assumed to be zero-mean Gaussian, actual error distributions differ somewhat from this ideal. Time-varying deterministic error sources, such as signal deformation, antenna phase-centre motion, and multipath, contribute

to unknown biases in the distribution mean. Random errors can also distort the actual error distribution. For example, diffuse multipath may result in heavy error-distribution tails. In addition to these physical sources of error, the empirical sampling process can also introduce distribution anomalies in the form of outliers.

Robust bounding of these distribution anomalies requires margin in overbound inflation. Since excess inflation reduces overall system availability, the most effective overbounding strategies are those that achieve conservative anomaly bounding for minimal protection-level inflation. Using the total inflation factor metric, Θ, this section evaluates the anomaly-performance of a range of overbounding strategies.

4.1 Overbounding Unknown Biases

Although common deterministic errors are removed in the differential correction process, remaining biases may still shift the error-distribution mean away from zero. The overbounding strategies discussed in Section 2 can all conservatively bound an unknown bias, given an appropriate amount of inflation. To assess bias-bounding performance, this section computes the total inflation, Θ, required for each method to overbound a particular normalized bias level, $\tilde{\mu} = \mu / \sigma$. This normalized bias parameter represents a maximum bound on the ratio of the pseudorange bias divided by broadcast σ for that pseudorange (which equals σ_{max} for sigma-relative bounding).

Of the overbounding methods described in Section 2, the paired-CDF overbound is the most efficient in bounding an unknown bias. This bound is ideal, in fact, in that there is no excess margin if the shift parameter equals the normalized bias (i.e. $\tilde{b} = \tilde{\mu}$). In this case, the maximum boundable normalized bias is found by solving (24) with $K = \xi = 1$:

$$\tilde{\mu} = (\Theta - 1) A_0 / \sqrt{N} \quad . \tag{26}$$

Analysis of bias performance for other overbounding strategies is more involved. For moment, EMC and EMP bounding, the maximum bias level, $\tilde{\mu}$, is computed by finding the shifted Gaussian error distribution that is tangent to the overbound at exactly one point. In moment bounding, for instance, the shifted actual error distribution is

$$m(t) = \int_{-\infty}^{\infty} e^{tx} \mathcal{N}(\mu, \xi\sigma_a) dx = e^{\frac{1}{2}(\xi\sigma_a t)^2 - \mu t} \quad . \tag{27}$$

For a given $\tilde{\mu}$, this equation grazes the overbound (11) at exactly one point. Solving for the tangent point provides an expression that relates $\tilde{\mu}$ to the parameters K and ξ. This relationship can be optimized, in turn, to find the parameter pair that results in the lowest overall inflation, Θ. The resulting expression for the maximum bias is:

$$\tilde{\mu} = \sqrt{\Theta^2 - \ln(\tfrac{1}{2} P_{HMI})} / \sqrt{N} \tag{28}$$

Similar analyses were performed for EMP bounding and for single-EMC bounding (with $\tilde{b} = 0$). Neither case resulted in a closed form solution for $\tilde{\mu}(\Theta)$. Instead, numerical solutions were obtained and plotted in Figure 4.

The figure presents $\tilde{\mu}(\Theta)$ performance both in an absolute form and in a relative form, normalized by the ideal bound, (26). The relative performance plot shows that the single-

EMC and EMP bounds provide very good bias bounding, quite close to that achieved by the ideal case of paired-CDF bounding. The relative performance of both single-EMC and EMP bounding decreases as the number of satellites, N, increases. In all cases, single-EMC bounding slightly outperforms EMP bounding. The EMC bounding case can be improved further, approaching the ideal paired-CDF level, by permitting paired-EMC bound ($\tilde{b} > 0$).

By comparison, moment bounding only provides efficient bias-bounding for large biases. Poor performance occurs for small biases because of the overhead of the inverse-moment transform, (10). For very large biases, however, moment-bounding performance surpasses single-EMC and EMP bounding performance. Figure 4 shows, for instance, that in the 25 satellite case moment bounding breaks even with EMP and single-EMC bounding near $\tilde{\mu}(\Theta)$ equal 0.5 (with Θ approximately 1.5). As $\tilde{\mu}(\Theta)$ increases further, moment bounding efficiency clearly approaches the ideal limit.

4.2 Heavy Tail Distributions

For some differential GNSS augmentation applications, particularly for GBAS, error distribution tails may roll off at a slower than Gaussian rate. These heavy tails introduce a significant obstacle for Gauss-based overbounding. In fact, the Gaussian forms for the overbounds described in Section 2 cannot conservatively bound heavy-tails. The problem is a fundamental one that relates to the definition of these bounds along the entire real line. At some extreme limit, a Gauss-based function always fails to overbound a heavy-tail distribution, regardless of the choice of the parameters K, ξ, and b. Thus, in general, an augmentation system must broadcast a non-Gaussian function to establish a formal overbound for a heavy-tail error distribution.

CDF bounds (both paired-CDF and EMC bounds) represent an exception to this generalization. With a small modification called core bounding, a Gaussian CDF bound can

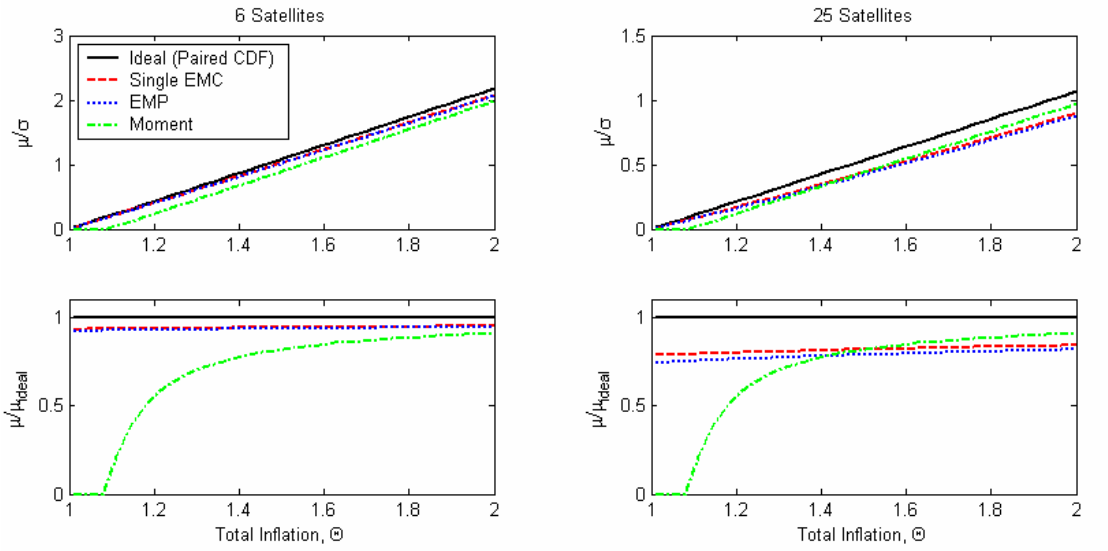

Figure 4. Maximum Bias as a Function of Inflation Factor.

be modified to compensate for heavier than Gaussian tails (Rife *et al.*, 2004b). Figure 5a illustrates this modification, which places a small fraction of P_{HMI} at infinity to permit a Gaussian to overbound a heavy-tail distribution, in this case a Laplacian (or double-exponential) distribution. The core bounding modification applies specifically to CDF-based bounding and, unfortunately, causes both EMP and moment bounds to diverge. In this sense, CDF-based bounding strategies have an advantage over other bounding strategies because a Gaussian overbound, rather than a non-Gaussian one, can be used to bound heavy tails.

Within the category of remaining overbounds, which includes both EMP and moment bounding, a further distinction can be drawn. Whereas an EMP bound always exists for any heavy-tail distribution, a moment bound only exists when heavy tails are less severe than exponential. For cases of exponential or heavier tails, the moment transform diverges. With the Laplacian distribution, for example, the moment transform is only defined along a fraction of the real axis.

$$m(t) = \begin{cases} \left(1 - \frac{1}{2}t^2\sigma^2\right)^{-1} & |t| < \sqrt{2}\sigma^{-1} \\ \infty & otherwise \end{cases} . \tag{29}$$

When tails are heavier-than-exponential, the moment transform, according to (9), diverges everywhere except at zero. Figure 5 illustrates this distinction between the EMP and moment bounds with the example of the Laplacian distribution. In both Figure 5b and 5c, the tails of the Laplacian distribution roll off more slowly than those of a Gaussian distribution. In the case of the EMP bound, however, the Laplacian distribution is well defined for all values of the error, x/σ. By contrast, the moment transform of the unity-variance Laplacian distribution is only defined between $\pm\sqrt{2}$.

Although a quantitative Θ analysis is not appropriate for the case of heavy-tail anomalies, overbounding alternatives can nevertheless be differentiated into three qualitative categories. The first category includes EMC and paired-CDF bounds. In this category, the core bounding approach can be applied to define a Gaussian overbound even when the actual distribution has heavy tails. A second category consists of EMP bounding, which permits bounding of any

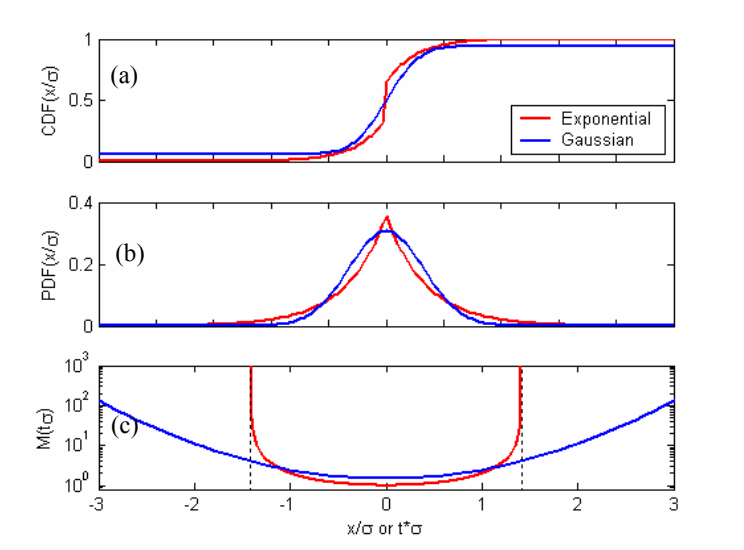

Figure 5. Bounding exponential distributions with (a) EMC or paired-CDF bounding (b) EMP bounding, or (c) moment bounding.

heavy-tail distribution using a non-Gaussian overbound with sufficiently heavy tails. The third and final category consists of moment bounding, which permits non-Gaussian bounding of heavy tail distributions, so long as the tails are not heavier than exponential.

4.3 Sample Sensitivity

Unknown biases and heavy distribution tails may result directly from the physics of the GNSS augmentation system. If the error bound is derived empirically, rather than through a physical model, additional anomalies may result from outliers in sampling.

This section quantifies the sensitivity of various overbounding strategies to sampled outliers using the total inflation metric, Θ. Overbounding strategies are compared on the basis of their robustness to a single outlier that falls at a location, x_o. Higher degrees of inflation are required to bound more extreme outliers, with larger values of x_o. Although sampling is random, by its nature, this section uses an approximate deterministic model to assess outlier sensitivity. Maximum allowable x_o values are computed assuming M samples, of which M-1 are assumed to exactly follow the nominal Gaussian distribution. The remaining outlier sample is modelled as a delta-spike at x_o. The PDF for this outlier model is:

$$g_{a,outlier} = \tfrac{M-1}{M}\mathcal{N}\left(0,\sigma_a\right)+\tfrac{1}{M}\delta\left(x-x_0\right) \quad . \tag{30}$$

This model expression immediately precludes EMP bounding, since the delta-function exceeds any PDF bound without an infinite total mass, K. Moment and EMC bounds (including the subset of paired-CDF bounds) are well defined, because each of these cases integrates over the delta function. For these strategies, maximum permissible x_o was found by searching the space of conservative bounds tangent to (30) at exactly one point.

Figure 6 summarizes the results, which were computed numerically. As illustrated in the figure, moment bounding is significantly less sensitive to extreme outliers than CDF bounding. Among the parameters for the EMC bound, the K and ξ were most effective in reducing outlier sensitivity. Thus, for a given level of inflation, the paired-CDF bound performed more poorly than the generic EMC approach with respect to outlier bounding. For all types of overbound, maximum x_o increases as the sample size, M, increases.

It should be noted that these results are dependent on the kernel function chosen to represent the outlier. Choosing a Gaussian kernel, rather than a delta-function kernel, actually enables

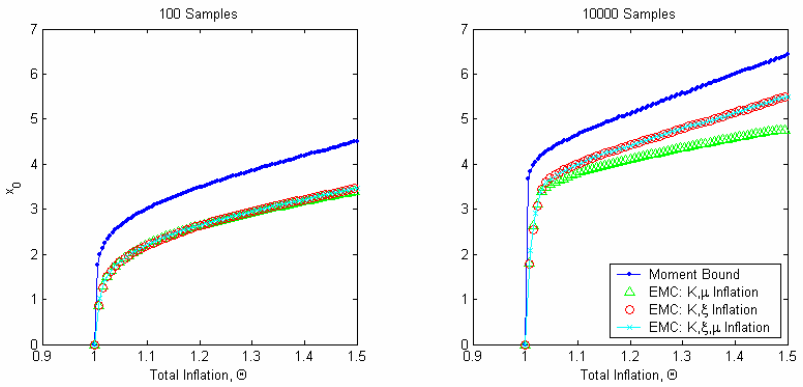

Figure 6. Sample Sensitivity

PDF bounding of the outlier model. Also, a Gaussian kernel improves x_o for CDF-based bounding and worsens x_o for moment bounding. Despite this dependence on kernel, the outlier model of (30) nonetheless provides general insight into the outlier-bounding sensitivity of various overbounding methods.

4.4 Synthesis

The previous sections examined the performance of various overbounding strategies in compensating for nonideal error distributions. The analysis took a general approach, assuming identical overbound parameters for all error distributions and ignoring restrictions on the number of parameters allowed by the bandwidth of the augmentation system's broadcast message. In the context of particular implementations of differential GNSS augmentation systems, these performance analysis tools could be applied to assess the relative benefits and penalties associated with each overbounding strategy. The trade space might, for instance, balance improved availability associated with tighter inflation, Θ, against the number of broadcast parameters required to implement a particular overbound. Alternatively, an analysis could explore the advantages of various overbounds given heterogeneous error sources. A companion paper, for instance, explores the advantages of EMP bounding for the case in which the geostationary satellite's unknown bias significantly exceeds the biases for other satellites in the GNSS constellation (Walter *et al.*, 2004)

For the generic case, assuming identical parameters for all satellites and neglecting bandwidth restrictions, the EMC strategy achieves the strongest overall level of performance. This method achieves ideal bounding of unknown biases, in the special case of paired-CDF bounding, for which $K = 1$. Similar performance is achieved for the more general EMC overbound, as long as total mass remains near unity. Furthermore, the EMC strategy, in contrast with other methods, permits Gaussian bounding of heavier-than-Gaussian tails using the core bounding approach. The weakest aspect of EMC bounding involves its outlier sensitivity, which is greater for EMC bounding than for moment bounding. An outlier removal technique might be required to implement an empirically based EMC bound.

5. SUMMARY

Overbounds provide a guarantee of integrity for safety-of-life GNSS augmentation systems. This paper introduces two new overbounding methods, called excess-mass CDF (EMC) and excess-mass PDF (EMP) overbounding. These methods, which conservatively represent nonideal error distributions, even those with asymmetry, multiple modes or nonzero mean, were compared to two existing overbounding approaches: paired CDF bounding and moment bounding. All strategies were compared on the basis of their robustness to distribution anomalies, including unknown biases, heavy tails, and sampled outliers. For the generic case, with equivalent overbounds for all satellites and with no bandwidth restrictions, the EMC bound achieved the best overall performance.

ACKNOWLEDGEMENTS: The authors gratefully acknowledge the Federal Aviation Administration for supporting this research. The opinions discussed here are those of the authors and do not necessarily represent those of the FAA or other affiliated agencies.

References

DeCleene B (2000) ***Defining Pseudorange Integrity – Overbounding***, Proceedings of ION GPS 2000, 1916-1924.

DeCleene B (2004) Personal Communication.

Golub GH and Van Loan CF (1996) ***Matrix Computations***, Johns Hopkins University Press, 52-53.

Ober PB, Farnsworth R, Breeuwer E, and van Willigen D (2001) ***SBAS Integrity Verification***, Proceedings of ION GPS 2001, 1805-1812.

Raytheon (2002) ***Algorithm Contribution to HMI for the Wide Area Augmentation System***, Raytheon Company Unpublished Work.

Rife J, Pullen S, Pervan B, and Enge P (2004a) ***Paired Overbounding and Application to GPS Augmentation,*** Proceedings IEEE Position, Location and Navigation Symposium, 439-446.

Rife J, Pullen S, Pervan B, and Enge P (2004b) ***Core Overbounding and its Implicatoins for LAAS Integrity,*** Proceedings of ION GNSS 2004.

Walter T, Blanch J, Rife J (2004) ***Treatment of Biased Error Distributions in SBAS***, Proceedings of the 2004 International Symposium on GPS/GNSS.

Appendix

This appendix proves that EMP overbounding is conservative through the range-to-position transformation. The position domain overbound is formed as a weighted sum of range-domain measurements. Before considering the N satellite proof, consider the case of two random variables, x and y, with distributions $f(x)$ and $g(y)$. The sum of these two random variables, $z = x + y$, has a distribution $h(z)$:

$$h(z) = \int_{-\infty}^{\infty} f(z-y)g(y)dy$$

On the condition that the functions f_{ov} and g_{ov} each overbound the corresponding range-domain error distributions according to (15), the convolution of these overbounds, $h_{ov}(z)$, is itself an overbound for the actual error distribution, $h(z)$.

$$h_{ov}(z) = \int_{-\infty}^{\infty} f_{ov}(z-y)g_{ov}(y)dy \geq \int_{-\infty}^{\infty} f(z-y)g(y)dy = h(z)$$

In the general GNSS augmentation case, there are N ranging measurements, one for each satellite. Each measurement is weighted by a sensitivity factor, S_i, which reflects projective geometry and variance-based weighting.

$$z = \sum_{i=1}^{N} S_i x_i$$

A position-domain overbound, $h_{ov}(z)$, can be derived by repeating the 2-measurement convolution proof N-1 times. This induction proof guarantees position-domain overbounding given EMP overbounding of the individual range-domain measurements.